MOLECULAR IMAGING AND BIOLOGY

RESEARCH ARTICLE

Detection of Hepatic Metastases Using Dual-Time-Point FDG PET/CT Scans in Patients with Colorectal Cancer

Jeong Won Lee,[1] Seok-Ki Kim,[2] Sang Mi Lee,[2] Seung Hwan Moon,[2] Tae-Sung Kim[2]

[1]*Department of Nuclear Medicine, Jeju National University Hospital, Jeju, Jeju Special Self-Governing Province, South Korea*
[2]*Department of Nuclear Medicine, National Cancer Center Research Institute and Hospital, 323 Ilsan-ro, Ilsandong-gu, Goyang-si, Gyeonggi-do 410-769, South Korea*

Abstract

Purpose: The purpose of this study was to determine the most useful parameter of dual-time-point 2-deoxy-2-[18F]fluoro-D-glucose positron emission tomography/computed tomography (PET/CT) for detection of hepatic metastases in patients with colorectal cancer.
Procedures: Thirty-nine patients had undergone a dual-time-point PET/CT scan and a subsequent histopathological confirmation for a workup of hepatic metastases. Detection rates were compared for visual analysis score, standardized uptake value (SUV), tumor-to-liver uptake ratio (TLR), and percent changes of the SUV and TLR.
Results: Of 91 liver lesions, 86 lesions were confirmed as metastases. The SUV and TLR of metastatic lesions on the delayed images were higher than those on the first scan ($p<0.001$). The signal-to-noise ratio of the delayed PET scan was higher than that of the first scan ($p<0.0001$). The TLR and SUV of the delayed scan showed the highest detection rates of 92% and 88%, whereas percent changes of SUV and TLR showed the lowest detection rates (51%, 67%). Visual analysis detected 87% on the delayed scan and 77% on the first scan.
Conclusions: A delayed scan is more favorable for the detection of hepatic metastases of colorectal cancer, and the TLR on the delayed scan was the most useful parameter.

Key Words: Dual-time-point, FDG, Positron emission tomography, Colorectal cancer, Liver metastasis

Significance: 2-Deoxy-2-[18F]fluoro-D-glucose (FDG) PET has been commonly used for detecting hepatic metastases in patients with colorectal cancer. However, FDG PET has limited detection ability for small-sized liver lesions or low metabolic lesions, which could be explained by the relatively high FDG uptake in normal liver tissue and the variable accumulation of FDG in metastatic lesions. For the improvement of the detection ability, a dual-time-point PET scan was designed and showed the high detection rate of liver tumors in several recent studies. However, it is still not clear which parameter of a dual-time-point scan is the most useful for the clinical identification of hepatic metastases. So, we intended to find the most useful parameter in the clinical use of the dual-time-point FDG PET. The results of our study showed that the tumor-to-liver ratio on the delayed PET scan, rather than the changes of FDG uptake and tumor-to-liver ratio, was the most useful parameter for the detection of hepatic metastases. Further, the delayed PET scan made the detection rate of hepatic metastases and signal-to-noise ratio increase.

Correspondence to: Seok-Ki Kim; *e-mail:* skkim@ncc.re.kr

Introduction

The liver is the most common site of metastasis in patients with colorectal cancer. Hepatic metastases are present in up to 25% of patients at the time of initial colorectal resection, and over 50% of patients with colorectal cancer eventually develop hepatic metastases [1]. Although surgical resection of hepatic metastases is a standard and a potential curative treatment, only a limited proportion of patients have undergone curative surgical resection of the hepatic lesions because of the large size and/or high number of metastatic lesions [2–5]. Hence, accurate analysis of hepatic metastatic lesions using non-invasive imaging modalities, such as ultrasonography,

computed tomography (CT), and magnetic resonance imaging (MRI), is necessary for the preoperative selection of patients.

2-Deoxy-2-[^{18}F]fluoro-D-glucose (FDG) positron emission tomography (PET) has been used for detecting hepatic metastases in patients with colorectal cancer and has demonstrated higher accuracy than contrast-enhanced CT images [6–9]. A previous meta-analysis study demonstrated that FDG PET was the most accurate for detection of colorectal liver metastases, with an overall sensitivity of 95% per-patient basis and 76% per-lesion basis [10]. However, recent studies have shown that the sensitivity of FDG PET for detecting hepatic metastases on a per-lesion basis was only 54–65%, suggesting a limited detection ability for small-sized lesions or low metabolic lesions [8, 11]; these results could be explained by the relatively high FDG uptake in normal liver and the variable accumulation of FDG in metastatic lesions [8, 12].

Recently, there have been several attempts to enhance the detection rate of malignant lesions with dual-time-point FDG PET scans [13–24]. According to previous studies, tumor tissue shows gradual accumulation of FDG, suggesting that the contrast between tumor and normal background tissue on delayed PET imaging could be higher than that on routine PET imaging [13, 14, 25]. Based on this characteristic of malignant lesions, dual-time-point FDG PET imaging demonstrated improved tumor detection in patients with lung cancer [15], breast cancer [16], gallbladder carcinoma [17], and thymic tumor [18]. Furthermore, there have been several studies to improve the detection of liver tumors using a dual-time-point PET scan [19–24], suggesting that a dual-time-point PET scan was useful for the detection of hepatic metastases. However, it is not clear which parameter of a dual-time-point scan is the most useful for the clinical identification of hepatic metastases.

The purpose of this study was to compare the diagnostic accuracies of various parameters of dual-time-point FDG PET in order to identify the most effective parameter for detecting hepatic metastases in colorectal cancer patients and to evaluate the clinical usefulness of a delayed PET scan.

Materials and Methods

Patients

Between June 2003 and December 2006, a total of 273 patients with colorectal cancer who underwent FDG PET/CT scans for the diagnostic workup of hepatic metastasis were retrospectively reviewed. Of them, 39 patients (29 men and ten women, mean age: 62±12 years, range: 28–81 years) were enrolled in this study according to the inclusion criteria as follows: (1) those who were diagnosed with colorectal cancer and had suspicion of hepatic metastases based on contrast-enhanced abdominal CT images, (2) those who underwent a dual-time-point FDG PET/CT scan for further workup of hepatic metastases, and (3) those who had a subsequent histopathological confirmation of all liver lesions that were suspicious for metastases. Of the 39 patients, 31 patients

(80%) had undergone imaging studies for the diagnostic workup of primary colorectal cancer (i.e., sigmoid colon cancer, ten patients; rectal cancer, nine patients; ascending colon cancer, three patients; rectosigmoid junction cancer, three patients; transverse colon cancer, two patients; descending colon cancer, one patient; and cecal cancer, one patient). The remaining eight patients (20%) had undergone imaging studies for suspicion of hepatic metastases after curative surgical resection of the primary colorectal cancer lesion (i.e., rectal cancer, three patients; sigmoid colon cancer, two patients; ascending colon cancer, one patient; transverse colon cancer, one patient; and descending colon cancer, one patient). After diagnostic imaging studies, histopathological confirmation was performed on all liver lesions. Patients were excluded from the study if they had (1) a previous history of another malignancy or (2) received any neoadjuvant therapy prior to operation or biopsy of the liver lesions.

FDG PET/CT Imaging

Dual-time-point FDG PET/CT was performed using a PET/CT scanner (Biograph LSO, Siemens Medical Systems). The dual-time-point PET/CT scan consisted first of the whole-body PET/CT scan and then the delayed regional PET/CT scan that focused on the liver. After the patients had fasted for at least 6 h, FDG (mean dose: 442.5±74.5 MBq) was intravenously administered. The first whole-body PET/CT scan, from the skull base to the femur, was performed 67±11 min (range: 45–86 min) after the FDG injection. We used a scout view with 30 mA and 130 kVp, followed by a spiral CT scan of the patient, whose arms were raised, using the following settings: effective amperage of 50 mA, 130 kVp, 5-mm section width, 4-mm collimation, 12-mm table feed per rotation, and 0.8 s per rotation. After the CT scans, the PET images were acquired at 3 min per bed position of 11.2 cm in the three-dimensional acquisition mode. The CT images were then reconstructed onto a 512 × 512 matrix and converted into 511-keV-equivalent attenuation factors for attenuation correction. The PET images were reconstructed onto a 128 × 128 matrix using ordered-subsets expectation maximization with an attenuation correction. The delayed regional PET/CT scan was performed 113±20 min (range: 80–165 min) after the FDG injection, and the mean-time intervals between the first and the delayed PET/CT scans were 52± 17 min (range: 35–100 min). Both whole-body and delayed regional PET/CT scans were performed using the same PET/CT scanner (Biograph LSO). The images of the delayed PET/CT scan were obtained at a 6-min per-bed position. All FDG PET/CT images were reconstructed into transaxial, coronal, and sagittal images.

Image Interpretation

Firstly, signal-to-noise ratios (SNRs) of the first and delayed PET/CT scans were measured to compare the image quality of both scans. The SNR was calculated according to the methods of a previous study by Masuda et al. [26]. The SNR of the liver in FDG PET images was defined as the mean of the standardized uptake values (SUVs) divided by the standard deviation (SD) [27]. A spheroid-shaped region of interest (ROI) was placed over non-tumorous liver tissue, and the mean and SD of the SUV of the normal liver tissue were measured. The same ROI was used for both the first and delayed scans. Contrast-enhanced CT images were used to draw the ROIs to allow for careful correlation and

exclusion of liver lesions. The mean of the volumes of the spheroid-shaped ROIs was 161 ± 63 cm^3.

After measuring the SNRs, the first and delayed PET images were visually assessed by two experienced nuclear medicine physicians in consensus. All liver lesions were assessed on the basis of a four-point scale by comparing the FDG uptake of the liver lesions to that of the surrounding normal liver tissue as follows: (1) score 1, definitely benign, the uptake of the lesion is less than or equal to that of normal liver tissue; (2) score 2, probably benign, the uptake of the lesion is slightly greater than that of normal liver, but the lesion is not seen in maximum intensity projection (MIP) images; (3) score 3, probably metastatic, the lesion of which the uptake is greater than that of the liver and is well-visualized in MIP images or the lesion of which the uptake is slightly greater than normal liver with definite liver lesion on the non-contrast enhanced CT images of PET/CT scan; and (4) score 4, definitely metastatic, the uptake of the lesion is much greater than that of the normal liver tissue.

Afterwards, the maximum SUV (SUVmax) and tumor-to-liver uptake ratio (TLR) of FDG on both the first and delayed scans were calculated for all liver lesions. The SUV was calculated as (decay-corrected activity [kBq] per milliliter of tissue volume)/(injected [^{18}F] FDG activity [kBq]/body mass [g]). The SUVmax of each lesion was obtained by placing a circular ROI manually at the site of the maximum FDG uptake on the transaxial images. In cases of liver lesions with score 1, ROIs were drawn on FDG PET images with careful correlation using contrast-enhanced liver CT and MRI images. By dividing the SUVmax of the liver lesions by the mean SUV of normal liver tissue, TLR were calculated for each liver lesion.

Histopathological Confirmation

Of the 39 patients included in this study, 38 patients (97%) had undergone radical surgical resection of suspected hepatic metastatic lesions, and the remaining one patient (3%) had undergone percutaneous needle biopsy of a liver lesion. All of the lesions that had been detected on contrast-enhanced CT or FDG PET/CT were histopathologically confirmed. The mean-time interval between the FDG PET/CT scan and surgical resection or biopsy was 10 ± 22 days. All specimens were reviewed by an experienced pathologist, and the size, number, and pathological grade of the metastatic liver lesions were determined. In the one patient who had undergone percutaneous needle biopsy, a metastatic liver lesion had been suspected based on a contrast-enhanced abdominal CT; however, the biopsy revealed active cirrhotic change with no evidence of metastasis. Therefore, for this patient, only the surgical resection of the primary colon cancer lesion was performed, without resection of the liver.

Statistical Analysis

The diagnostic accuracies of eight parameters of dual-time-point FDG PET scans, which included (1) the visual analyses scores, (2) SUVmax, and (3) TLR of the first PET scans; (4) the visual analyses scores, (5) SUVmax, and (6) TLR of the delayed PET scans; and (7) percent changes of SUVmax and (8) percent change of the TLR between the first and delayed scans, were compared using receiver operating characteristic (ROC) curve analysis with a calculation of the area under the ROC curve (AUC). Paired t tests and Wilcoxon signed-rank tests were applied to determine the statistical differences between the two scans with respect to the SNRs and mean SUV of the liver, SUVmax, and TLR of the liver

lesions. All these analyses were performed using MedCalc v. 10.1 software (MedCalc software, Mariakerke, Belgium), and p values of less than 0.05 were considered to be statistically significant.

Results

Histopathological Results

A total of 91 hepatic lesions were detected in 39 patients with colorectal cancer. Of the 91 lesions, 86 lesions in 34 patients were histopathologically proven to be hepatic metastatic lesions: (1) moderately differentiated type adenocarcinoma, 27 patients with 74 lesions; (2) well-differentiated type adenocarcinoma, four patients with eight lesions; (3) poorly differentiated type adenocarcinoma, two patients with three lesions (Fig. 1); and (4) mucinous carcinoma, one patient with one lesion. The remaining five lesions in five patients proved to be benign: (1) hemangioma, two patients (Fig. 2); (2) benign simple cyst, one patient; (3) organizing abscess, one patient; and (4) active cirrhotic change, one patient. The mean size of all the liver lesions was 1.6 ± 1.4 cm (range: 0.3–11.0 cm). Furthermore, 73 lesions (80%) were less than 2 cm and 33 lesions (36%) were less than 1 cm in maximum diameter.

The Changes of the SNR, SUVmax, and TLR on the Delayed Scan

The mean value of SNRs in the liver on the delayed PET/CT scan (11.7 ± 4.1) was significantly higher than that on the first whole-body PET/CT scan (8.7 ± 2.4, $p<0.0001$). Overall, the SNR of the delayed scan showed an increase of $34\pm31\%$ when compared to that of the first scan. Out of 39 patients, the delayed PET images of 36 patients (92%) showed an increase of the SNR; meanwhile, the remaining three patients (8%) showed a slight decrease of the SNR. Furthermore, the mean SUV of non-tumorous liver tissue on the delayed scans (1.9 ± 0.3) was slightly but significantly lower than that of the first scans (2.0 ± 0.3; $p<0.0001$).

The mean values of the SUVmax and TLR of the 86 metastatic lesions and five benign lesions on the first and delayed PET/CT scans are shown in Table 1. The mean values of the SUVmax and TLR of metastatic lesions on the delayed PET/CT scan were significantly higher than those on the first scan ($p<0.001$ for all). In contrast, there were no significant differences between the two scans in the SUVmax and TLR of benign lesions ($p>0.05$).

Of the 86 metastatic liver lesions, 70 lesions (81%) showed an increase of the SUVmax on the delayed scan compared to the first scan (mean percent change: $+24\pm25\%$), and one lesion (1%) showed no change of the SUVmax, whereas the remaining 15 lesions (18%) showed a decrease of the SUVmax (mean percent change: $-10\pm15\%$). Moreover, of the 86 metastatic lesions, 79 lesions (92%) showed an increase of the TLR on the delayed scan compared to the first scan (mean percent change: $+31\pm$
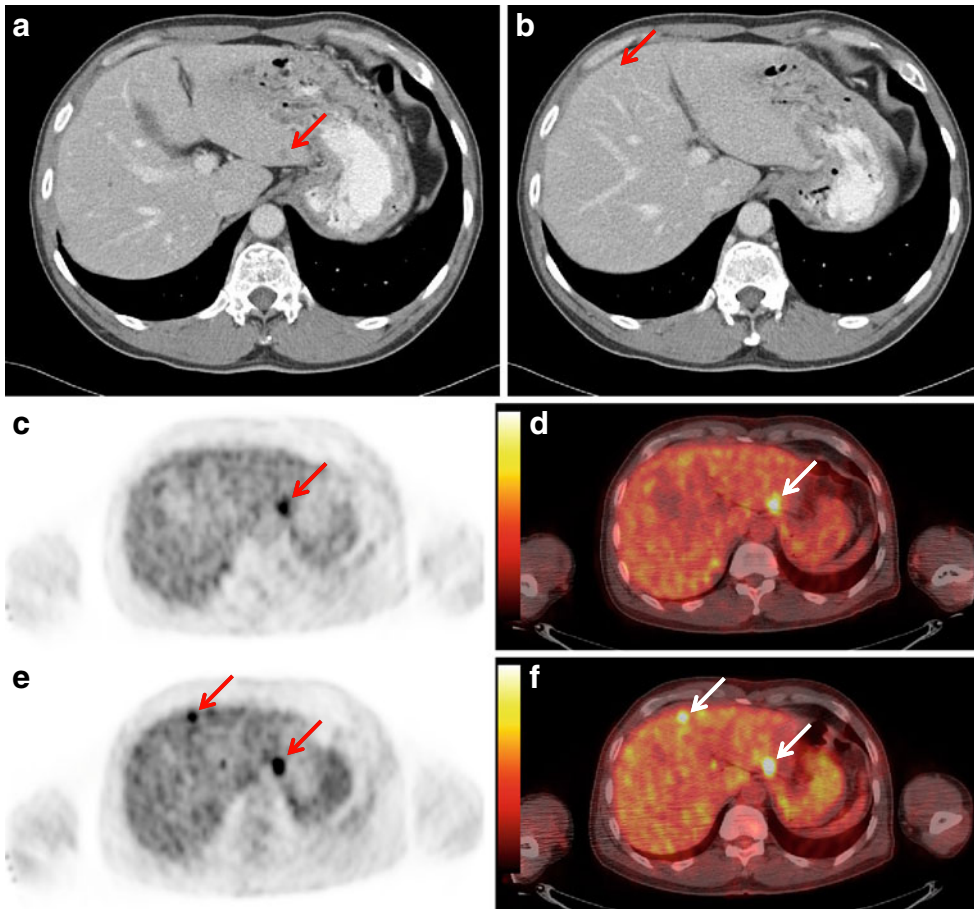
Fig. 1. Contrast-enhanced CT and the first whole-body and delayed regional FDG PET/CT images of a 58-year-old male patient with rectal cancer. The contrast-enhanced CT images (**a**, **b**) show small low-attenuated lesions in the liver, left medial (0.5-cm-sized) and lateral (0.8-cm-sized) segments, suspicious of hepatic metastatic lesions. The first whole-body FDG PET (**c**) and fused PET/CT (**d**) images showed a focal hypermetabolic lesion in the left medial segment with a maximum SUV of 7.11 and tumor-to-liver (T/L) uptake ratio of 3.32, suggesting a metastatic lesion; however, no definite abnormal hypermetabolic lesion is seen in the left lateral segment. In the delayed regional liver PET (**e**) and fused PET/CT (**f**) images, two foci of hypermetabolic lesions are observed in the liver: medial segment (maximum SUV: 7.94, TLR: 3.91) and lateral segment (maximum SUV: 5.52, TLR: 2.72). These two lesions were histopathologically diagnosed as metastatic lesions from rectal cancer.

29%), while seven lesions (8%) showed a decrease of the TLR (mean percent change: $-14 \pm 18\%$). Each of these seven lesions also showed a decrease of the SUVmax. Of these seven lesions, the SUVmax and TLR of two lesions were decreased over 30% (SUVmax: -54% and -39%, respectively; TLR: -48% and -31%, respectively), because of respiratory motion artifact of the patients.

Comparison of Detection Rate by Visual Analysis

The results of the visual analyses using the four-point scale of the first and delayed PET/CT scans for the detection of hepatic metastases are shown in Table 2. On the first scan, the detection rate of metastatic lesions was 77% (66 of 86 metastatic lesions, which were assessed as score 3 or 4); on the delayed scan, 87% (75 of 86 lesions) of metastatic lesions were detected. In nine lesions that were newly detected on the

delayed scan, the average size was 0.6 ± 0.2 cm (range: 0.3–1.0 cm); of those, eight lesions were less than 1 cm. Further, the average sizes of the metastatic lesions which were not detected on the first scan (20 lesions) and the delayed scan (11 lesions) were 0.7 ± 0.3 cm (range: 0.3–1.5 cm) and 0.8 ± 0.3 cm (range: 0.5–1.5 cm), respectively.

The AUC of visual analysis on the delayed PET/CT scan (0.910, 95% CI: 0.833–0.960; Fig. 3b) was higher than that of the first PET/CT scan (0.856, 95% CI: 0.768–0.920; Fig. 3a); however, no statistical significance was noted between the AUC of both scans ($p > 0.05$). All five benign liver lesions were categorized as score 1 on the visual analyses of the first scan, and four of the five lesions were categorized as score 1 on the visual analyses of the delayed scan. The remaining one lesion, which was histopathologically confirmed as a benign hemangioma, was categorized as score 2 on the delayed scan (Fig. 2). However, the lesion
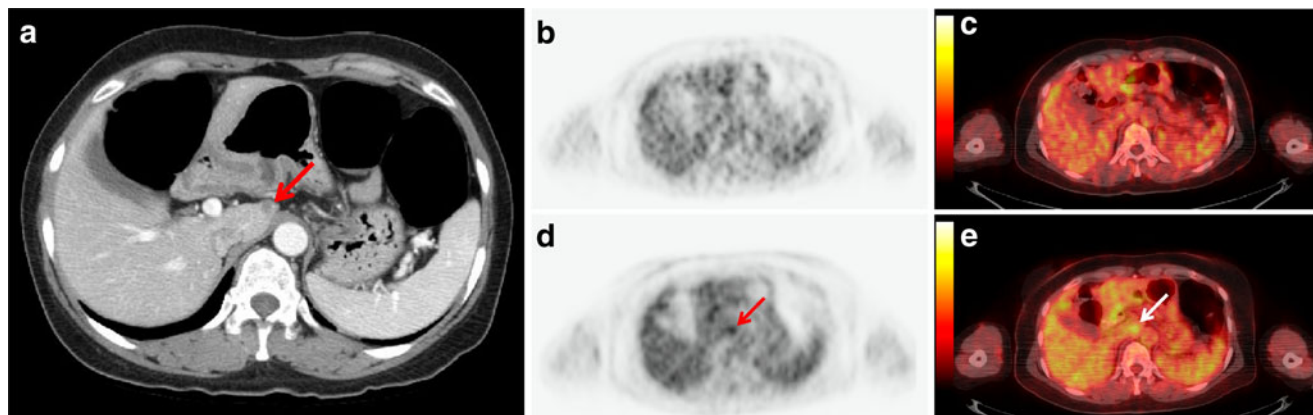
Fig. 2. Contrast-enhanced CT and the first whole-body and delayed regional FDG PET/CT images of a 50-year-old female patient with sigmoid colon cancer. In the contrast-enhanced CT image (**a**), 0.9-cm-sized, low-attenuated lesion is observed in the caudate lobe of the liver, suspicious for a metastatic lesion. The first whole-body FDG PET (**b**) and fused PET/CT (**c**) images show no evidence of an abnormal focal hypermetabolic lesion in the caudate lobe of the liver. In the delayed regional liver PET (**d**) and fused PET/CT (**e**) images, mild focal FDG uptake is seen in the caudate lobe with a maximum SUV of 2.38 and tumor-to-liver ratio of 1.38. The lesion of the caudate lobe was histopathologically diagnosed as a hemangioma.

was still classified as benign lesion because only the lesions with score 3 or more were assessed as metastatic lesions.

Comparison of Parameters from Dual-time-point PET/CT

Among the various parameters of dual-time-point PET scan, the TLR on the delayed PET scan was found to be the most useful parameter with a detection rate of 92%, detecting 79 of 86 metastatic lesions. The detection rate and AUC of eight parameters of the dual-time-point PET scan for the detection of hepatic metastasis are shown in Table 3. All five benign liver lesions were assessed as benign lesions by each parameter of the dual-time-point PET scan, showing a 0% false-positive rate in all eight parameters. Of the eight parameters of dual-time-point FDG PET, the TLR on the delayed PET scan shows the highest AUC (0.964, 95% CI: 0.902–0.992; Fig. 3c), with a detection rate of 92%, by using the best cutoff value of 1.4. In contrast, the percent change of the SUVmax and TLR showed a much lower AUC and

lower detection rate (51% and 67%, respectively) than other parameters of FDG PET.

Discussion

The results of our present study demonstrated that using a delayed PET scan with longer emission time increased the detection rate of hepatic metastases. The TLR on the delayed PET scan was the most accurate parameter among the various parameters of dual-time-point FDG PET for detection of hepatic metastases. Further, over 90% of hepatic metastatic lesions showed increased TLR on the delayed PET scan, and there were significant increases of the SUVmax in the metastatic lesions and the SNR on the delayed PET images.

In the present study, we showed that the TLR on the delayed PET scan is the most useful of various parameters by dual-time-point PET scan for the detection of hepatic metastasis. In previous studies performed for detection of liver tumors by dual-time-point FDG PET scan, visual

Table 1. The mean values of the SUVmax and TLR of 91 liver lesions (86 metastatic lesions, five benign lesions) on the first whole-body scan and delayed regional PET/CT scan

		First scan	Delayed scan	p value
Metastatic lesions (n=86)	SUVmax	6.0±3.5	7.0±4.4	<0.001[a]
	% change of SUVmax		+17±27%	
	TLR	3.1±1.9	3.9±2.6	<0.001[a]
	% change of TLR		+27±31%	
Benign lesions (n=5)	SUVmax	2.3±0.3	2.4±0.3	0.3[b]
	% change of SUVmax		+4±8%	
	TLR	1.2±0.2	1.2±0.2	0.6[b]
	% change of TLR		+2±9%	

[a]Paired t test
[b]Wilcoxon signed-rank test

Table 2. The results of visual analyses of 91 liver lesions (86 metastatic lesions, five benign lesions) on the first whole-body scan and delayed regional PET/CT scan on the basis of a four-point scale

Visual analysis score	No. of lesions ($n=91$)	
	First scan	Delayed scan
1	20	10
2	5	6
3	17	9
4	49	66
p value[a]	0.02	

[a]Chi-square test for trend

analysis was the main parameter used to detect liver tumors [20–22, 24, 25]. In contrast to previous studies, we performed ROC curve analysis to determine the most effective of various parameters, including visual analysis, of dual-time-point PET scan. Among eight parameters of dual-time-point PET scan, the TLR on the delayed PET scan had the highest accuracy in the detection of hepatic metastasis, with a detection rate of 92% and with no false-positive findings. In contrast, the percent changes of the SUVmax and TLR had lower values of AUC than other parameters, suggesting that, in the detection of hepatic metastases, the TLR on the delayed scan can be more helpful than the change of FDG uptake between the first and delayed PET scans. However, because of the small number of benign liver lesions, further studies are needed to elucidate the use of the TLR on the delayed PET scan.

We performed the delayed regional PET/CT scan with a longer emission scan time (6 min) than that of a standard PET/CT scan, demonstrating the significant increase of the SNR, which is representative of image quality. Because the total examination time was limited, the emission scan time of the whole-body PET/CT scan in our study was only 3 min per bed position. Although delayed imaging may suffer from

high noise owing to the radioactive decay of ^{18}F [13], a previous study has shown that, by using a longer emission scan time on spot images than that used on whole-body images, the quality of the spot images was better than that of the whole-body images, and the SNR of the spot images was higher than that of the whole-body images [28]. Furthermore, a previous study by Masuda et al. [26] showed that PET images with a longer emission scan time improved the image quality of PET scan and did not increase the necessary dose of injected FDG. The delayed PET scan images with longer emission scan time in our study also showed an increase of the SNR, indicating a better image quality than that of the first whole-body PET/CT scan.

The improvement of tumor-to-background contrast of the delayed PET scan could be more helpful in detecting small hepatic metastatic lesions, as well as improving image quality. Although the results of our study and previous studies [21, 22, 25] have demonstrated a slight decrease of the mean SUV of normal liver tissue on the delayed PET scan, a recent study by Chin et al. [29] showed that there was no significant difference in hepatic activity between 1- and 3-h FDG PET images, suggesting that improvements in tumor image contrast with delayed imaging may be primarily due to cumulative FDG uptake within the tumor rather than reduction in normal liver activity. In the present study, there was no obvious histopathological characteristic of the hepatic lesions that was newly detected on the delayed PET scan. Meanwhile, 89% (eight out of nine lesions) of newly detected metastatic lesions by visual analysis on the delayed PET scan was less than 1 cm, suggesting that a delayed PET scan with longer emission scan time could be more helpful in delineating small-sized lesions. Hence, hepatic evaluation using the first whole-body PET scan might be insufficient to detect hepatic metastatic lesions of small size or low metabolism.

Similar to the results of a previous study by Dirisamer et al. [22], we found that a delayed hepatic regional PET scan
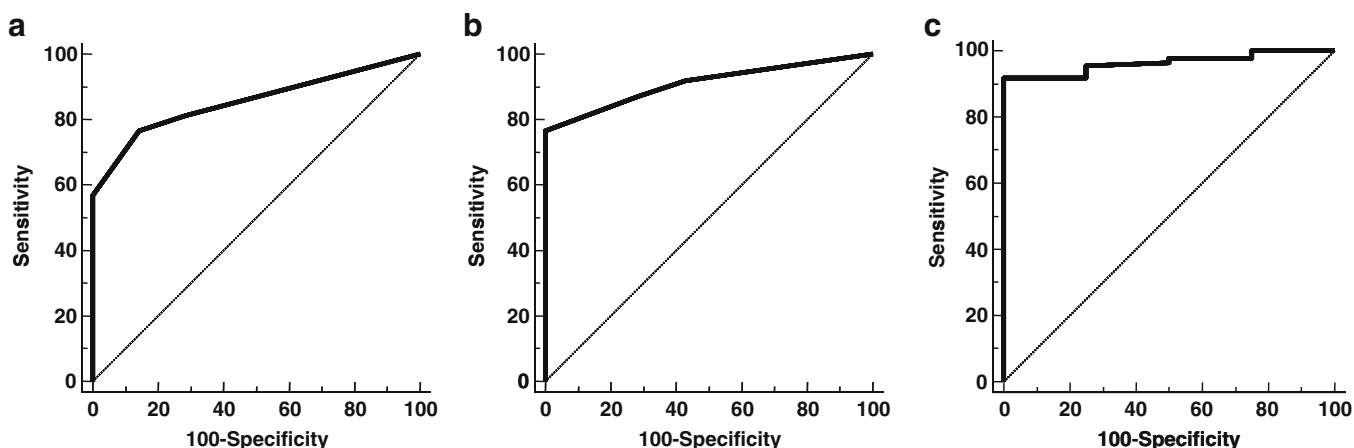

Fig. 3. ROC curve of visual analysis using four-point scale on the first (**a**) and delayed (**b**) FDG PET/CT scans and ROC curve of TLR on the delayed FDG PET/CT (**c**).

Table 3. The detection rate and area under the ROC curve (AUC) of various parameters of dual-time-point FDG PET for the detection of hepatic metastasis

Parameter	Cutoff value	Detection rate (%)	AUC (95% CI)
Visual analysis of the first scan		77	0.856 (0.768–0.920)
Visual analysis of the delayed scan		87	0.910 (0.833–0.960)
SUVmax of the first scan	2.5	86	0.922 (0.847–0.968)
SUVmax of the delayed scan	2.6	88	0.922 (0.847–0.968)
TLR of the first scan	1.4	85	0.922 (0.847–0.968)
TLR of the delayed scan	1.4	92	0.964 (0.902–0.992)
% change of SUVmax	13.3	51	0.664 (0.557–0.759)
% change of TLR	13.0	67	0.779 (0.680–0.859)

could improve the lower sensitivity of the first whole-body PET scan. According to our study, there was a significant increase of the SUVmax and TLR of metastatic lesions and decrease of the mean SUV of normal liver tissue in the delayed PET/CT images. Further, there were no significant differences between the SUVmax and TLR of the five benign lesions on the delayed PET/CT images, although the number of benign lesions was too small. The detection rate of the metastatic lesions on the first PET scan by visual analysis in our study was 77%, which is similar to the results of a previous meta-analysis study [10]. By using the delayed regional PET/CT scan in our study, the detection rate of metastatic lesions increased by only 10%, which is lower than that (31%) of a previous study by Dirisamer et al. [22]. However, they showed a lower sensitivity of the first whole-body PET/CT scan (59%) than that found by of other previous studies and by our study; this may be from the various types of primary malignant tumors studied.

There were several limitations in the present study. First, there was a selection bias. The patients in our study were selected based on certain criteria, and not all patients with colorectal cancer who had hepatic metastases were enrolled. Because of the clinical condition of the patients, the histopathological confirmation of all suspected hepatic metastatic lesions was performed in only a small number of patients. Second, only the diagnostic performance of the dual-time-point FDG PET/CT was evaluated in the present study, and the effects of the differences in clinical management of the patients were not evaluated. The studies that were aimed at the assessment of the accuracy of detection are subject to bias and may lead to an overestimation of the clinical value of FDG PET [30]. Hence, further prospective randomized studies are needed to evaluate the clinical value of the dual-time-point PET/CT scan. Third, there was a wide range of time-points (80–165 min) for the delayed PET scan because of the clinical condition of the patients, although we tried to perform the delayed scan at 2 h after the injection of FDG. Many previous studies have performed the delayed FDG PET scan around 2 h after the injection of FDG [17, 18, 21, 22, 31, 32] or around 3 h after the injection [16, 19]; however, no optimized delayed scan time-point has yet been recommended. According to a previous study by Chen et al. [33], the diagnostic value of a 110-min scan imaging was higher than that of a 233-min scan imaging.

Conclusion

The use of the delayed PET/CT scan increased the detection rate of hepatic metastatic lesions in patients with colorectal cancer. Also, the TLR on the delayed PET scan, rather than the changes of the SUVmax and TLR, was the most useful parameter for the detection of hepatic metastases. The SNR, which could represent the image quality of the PET scan, was also significantly increased on the delayed images. Therefore, the delayed FDG PET scan with a longer emission scan time could provide good-quality images and help in the detection of hepatic metastases.

Conflicts of Interest. The authors declare that they have no conflicts of interest.

References

1. Taylor I (1996) Liver metastases from colorectal cancer: lessons from past and present clinical studies. Br J Surg 83:456–460
2. Gayowski TJ, Iwatsuki S, Madariaga JR et al (1994) Experience in hepatic resection for metastatic colorectal cancer: analysis of clinical and pathologic risk factors. Surgery 116:703–710
3. Jatzko GR, Lisborg PH, Stettner HM, Klimpfinger MH (1995) Hepatic resection for metastases from colorectal carcinoma–a survival analysis. Eur J Cancer 31A:41–46
4. Nakamura S, Suzuki S, Baba S (1997) Resection of liver metastases of colorectal carcinoma. World J Surg 21:741–747
5. Scheele J, Stangl R, Altendorf-Hofmann A, Gall FP (1991) Indicators of prognosis after hepatic resection for colorectal secondaries. Surgery 110:13–29
6. Delbeke D, Vitola JV, Sandler MP et al (1997) Staging recurrent metastatic colorectal carcinoma with PET. J Nucl Med 38:1196–1201
7. Zhuang H, Sinha P, Pourdehnad M, Duarte PS, Yamamoto AJ, Alavi A (2000) The role of positron emission tomography with fluorine-18-deoxyglucose in identifying colorectal cancer metastases to liver. Nucl Med Commun 21:793–798
8. Rappeport ED, Loft A, Berthelsen AK et al (2007) Contrast-enhanced FDG-PET/CT *vs.* SPIO-enhanced MRI *vs.* FDG-PET *vs.* CT in patients with liver metastases from colorectal cancer: a prospective study with intraoperative confirmation. Acta Radiol 48:369–378
9. Kim BI (2008) Clinical application of F-18 FDG PET (PET/CT) in colorectal and anal cancer. Nucl Med Mol Imaging 42(Supple):52–59
10. Bipat S, van Leeuwen MS, Comans EF et al (2005) Colorectal liver metastases: CT, MR imaging, and PET for diagnosis–meta-analysis. Radiology 237:123–131
11. Ruers TJ, Langenhoff BS, Neeleman N et al (2002) Value of positron emission tomography with [F-18]fluorodeoxyglucose in patients with colorectal liver metastases: a prospective study. J Clin Oncol 20:388–395

12. Brix G, Ziegler SI, Bellemann ME et al (2001) Quantification of [(18)F] FDG uptake in the normal liver using dynamic PET: impact and modeling of the dual hepatic blood supply. J Nucl Med 42:1265–1273

13. Kubota K, Itoh M, Ozaki K et al (2001) Advantage of delayed whole-body FDG-PET imaging for tumour detection. Eur J Nucl Med 28:696–703

14. Zhuang H, Pourdehnad M, Lambright ES et al (2001) Dual time point 18F-FDG PET imaging for differentiating malignant from inflammatory processes. J Nucl Med 42:1412–1417

15. Yen RF, Chen KC, Lee JM et al (2008) 18F-FDG PET for the lymph node staging of non-small cell lung cancer in a tuberculosis-endemic country: is dual time point imaging worth the effort? Eur J Nucl Med Mol Imaging 35:1305–1315

16. Kumar R, Loving VA, Chauhan A, Zhuang H, Mitchell S, Alavi A (2005) Potential of dual-time-point imaging to improve breast cancer diagnosis with (18)F-FDG PET. J Nucl Med 46:1819–1824

17. Nishiyama Y, Yamamoto Y, Fukunaga K et al (2006) Dual-time-point 18F-FDG PET for the evaluation of gallbladder carcinoma. J Nucl Med 47:633–638

18. Inoue A, Tomiyama N, Tatsumi M et al (2009) (18)F-FDG PET for the evaluation of thymic epithelial tumors: Correlation with the World Health Organization classification in addition to dual-time-point imaging. Eur J Nucl Med Mol Imaging 36:1219–1225

19. Koyama K, Okamura T, Kawabe J et al (2002) The usefulness of 18F-FDG PET images obtained 2 hours after intravenous injection in liver tumor. Ann Nucl Med 16:169–176

20. Lin WY, Tsai SC, Hung GU (2005) Value of delayed 18F-FDG-PET imaging in the detection of hepatocellular carcinoma. Nucl Med Commun 26:315–321

21. Dirisamer A, Halpern BS, Schima W et al (2008) Dual-time-point FDG-PET/CT for the detection of hepatic metastases. Mol Imaging Biol 10:335–340

22. Chen YK, Kao CH (2005) Metastatic hepatic lesions are detected better by delayed imaging with prolonged emission time. Clin Nucl Med 30:455–456

23. Kuker RA, Mesoloras G, Gulec SA (2007) Optimization of FDG-PET/CT imaging protocol for evaluation of patients with primary and metastatic liver disease. Int Semin Surg Oncol 4:17

24. Arena V, Skanjeti A, Casoni R, Douroukas A, Pelosi E (2008) Dual-phase FDG-PET: delayed acquisition improves hepatic detectability of pathological uptake. Radiol Med 113:875–886

25. Hamberg LM, Hunter GJ, Alpert NM, Choi NC, Babich JW, Fischman AJ (1994) The dose uptake ratio as an index of glucose metabolism: useful parameter or oversimplification? J Nucl Med 35:1308–1312

26. Masuda Y, Kondo C, Matsuo Y, Uetani M, Kusakabe K (2009) Comparison of imaging protocols for 18F-FDG PET/CT in overweight patients: optimizing scan duration *versus* administered dose. J Nucl Med 50:844–848

27. Halpern BS, Dahlbom M, Auerbach MA et al (2005) Optimizing imaging protocols for overweight and obese patients: a lutetium orthosilicate PET/CT study. J Nucl Med 46:603–607

28. Tamaki T, Naito A, Nishio M, Kawahara K (2004) FDG-PET for evaluation of recurrent lymph node metastases in patients with surgically resected breast cancer: adding spot images to whole body images. Breast Cancer 11:60–64

29. Chin BB, Green ED, Turkington TG, Hawk TC, Coleman RE (2009) Increasing uptake time in FDG-PET: standardized uptake values in normal tissues at 1 *versus* 3 h. Mol Imaging Biol 11:118–122

30. Ruers TJ, Wiering B, van der Sijp JR et al (2009) Improved selection of patients for hepatic surgery of colorectal liver metastases with (18)F-FDG PET: a randomized study. J Nucl Med 50:1036–1041

31. Matthies A, Hickeson M, Cuchiara A, Alavi A (2002) Dual time point 18F-FDG PET for the evaluation of pulmonary nodules. J Nucl Med 43:871–875

32. Suga K, Kawakami Y, Hiyama A et al (2009) Dual-time point 18F-FDG PET/CT scan for differentiation between 18F-FDG-avid non-small cell lung cancer and benign lesions. Ann Nucl Med 23:427–435

33. Chen YM, Huang G, Sun XG et al (2008) Optimizing delayed scan time for FDG PET: comparison of the early and late delayed scan. Nucl Med Commun 29:425–430